Mathematical Modelling of Rice Gelatinisation and Dissolution in Beer Production

Accepted for publication in the American Institute of Chemical Engineers (AIChE) Journal, March 2002.

Malcolm J. Davey
Department of Mathematics and Statistics, University of Melbourne,
Victoria 3010, AUSTRALIA
email: m.davey@ms.unimelb.edu.au

Kerry A. Landman [1]
Department of Mathematics and Statistics, University of Melbourne,
Victoria 3010, AUSTRALIA
email: k.landman@ms.unimelb.edu.au

Mark J. McGuinness
School of Mathematical and Computing Sciences, Victoria University of Wellington,
Wellington, NEW ZEALAND
email: Mark.McGuinness@mcs.vuw.ac.nz

Hong N. Jin
BrewTech, Carlton & United Breweries Limited,
Foster's Brewing Group, Abbotsford, Victoria 3067 AUSTRALIA
email: hong.jin@cub.com.au

Keywords: nonlinear diffusion, starch, cooking, mass transfer, gelatinisation, dissolution

[1]author to whom correspondence should be addressed

Abstract

When beer is brewed in Asia, rice is traditionally used as an adjunct to provide additional sugars for the fermentation process. Under sufficiently high temperatures the grain, which is primarily composed of starch, takes up water. The starch undergoes a gelatinisation reaction when the moisture content is sufficiently high. Stirring and enzyme activity facilitate the removal of the outer gelatinised rice layers and this starch dissolves into solution. The starch molecules are subsequently broken down by enzymes. In this paper the water uptake, gelatinisation and dissolution processes are modelled using a modified diffusion approach. The mass of starch molecules dissolved in solution as the cooking proceeds is determined. The modelling results indicate that the dissolution process increases the speed of gelatinisation and that the gelatinisation front speed is a constant with time. The modelling takes into account different temperature regimes and a distribution of rice size. Such models help in understanding and optimising the total dissolved solids from this cooking process.

Introduction

During the beer-making process, adjuncts are generally used to supplement malt starch. In Asia rice is traditionally used as an adjunct to provide additional sugars because it is less expensive and readily available compared to cane sugar.

Rice is milled to produce small particles known as grist. The grist is placed into a rice cooker with large quantities of hot water and the mixture is kept well–stirred. The jacket of the cooker is heated so that the temperature of the mixture rises from around 60°C to 100°C and is held at this temperature for a certain period of time. During this process the grist, primarily composed of starch, takes up water and swells. The starch undergoes what is called a gelatinisation reaction. The shearing effects of stirring remove the gelatinised outer layers and these long-chained starch molecules dissolve into solution, where they are broken up into smaller-chained molecules by enzymes. Enzyme action may also enhance the breakdown and removal of the surface starch molecules. The dissolved starch product is added to another vessel, called the mash tun, to supplement the total amount of sugars obtained from the cooking of malt grist in the presence of malt enzymes.

In this paper, we present two models which estimate the mass of starch molecules dissolved as the cooking proceeds. The mathematical modelling is intended to improve understanding of the rice cooking process so the amount of dissolved starch solids can be optimised. Combining mathematical models and process know-how, optimisation of the total dissolved solids (i.e. yield extract) could be delivered by appropriate choices of the temperature regime, water-to-grist ratio, rice variety, and the size distribution of grist.

Within an individual rice particle, various processes occur during cooking. The heating, water uptake and swelling of the rice particle all involve diffusive processes. When water is present at sufficiently high temperatures, the starch undergoes a gelatinisation reaction and this can be incorporated into the water uptake models. Due to the constant stirring, after gelatinisation the cooked starch molecules are free to dissolve into the liquid medium. Determining the mass of the dissolved starch is our major task. No attempt is made to include the liquefaction process, whereby the dissolved starch undergoes molecular weight reduction by enzymes.

We first focus on understanding all of these processes in a single rice particle. These models are then generalised to account for a distribution of grist sizes. A limited sensitivity analysis on temperature regimes and particle size distribution is also undertaken.

Water uptake and gelatinisation

In this section a mathematical model for water uptake and gelatinisation is developed for a single rice particle, which draws on earlier approaches (McGowan and McGuinness, 1996; McGuinness et al., 1998; McGuinness et al, 2000). Asymptotic methods are used to determine the swelling size of the rice particle and the boundary between the cooked and uncooked portions of the particle. We first describe some characteristics of rice (using Juliano (1985) as a major reference) and experimental studies of the processes in rice cooking.

Background to the modelling

A rice grain is primarily composed of starch, with small amounts of proteins, lipids and water. The endosperm is the largest component of the rice grain and the richest in starch. This endosperm is surrounded by many thin bran layers. To produce grist for brewing, the rice is milled to remove these bran layers and break up the endosperm into smaller pieces, around 0.1 to 1.5 mm in size. Depending on the level of milling, about 90% of the dry mass of milled rice is made up of starch. The rice particles are assumed to be spherical in shape.

The starch is enclosed in granules, which are embedded in a protein matrix. The granules are usually 3-9μm in diameter. There are two types of starch polymers – amylose and amylopectin. Amylose consists mainly of a linear chain, whereas amylopectin has many branching polymer chains and has a more "tree-like" structure. Depending on rice variety, some starch granules are almost entirely composed of amylopectin, whereas others can be quite high in amylose. The organizational structure of these two starch molecules within a granule is complex. Differences between the two types of starch polymers will be ignored here.

Rice cooking is a common word for describing the starch gelatinisation reaction. This occurs in the presence of sufficient water when the temperature is high enough. Studies of the heating, water uptake and gelatinisation processes are now discussed together with their implications for the modelling.

Experimental work for water hydration of grains (Fortes et al., 1981; Kustermann et al., 1981) and recent modelling work (McGowan and McGuinness, 1996) concentrating on a single cereal grain have demonstrated that the conductive heating process proceeds far more rapidly than the hydrating process. Therefore, heat conduction within the grist is negligible and the internal temperature of every rice particle can be taken to be the bulk temperature.

Water motion within a rice particle is driven by a chemical potential gradient which can

be written in terms of water activity. This framework gives rise to a Fickian diffusion model for the water uptake. As the water is absorbed by the rice particle, the starch will swell to accomodate the additional water.

Many rice studies have concentrated on the soaking of rice grains at fixed temperatures (Suzuki etal., 1977; Takeuchi, 1997a; Zhang et al., 1975) or the parboiling process (Bakshi and Sing, 1982; Kar et al., 1999). For temperatures below 50°C, the grains absorb a limited amount of water up to approximately 30% moisture content (wet basis). The resulting grains are not cooked because the starch has not undergone gelatinisation. From common experience with small samples, it is known that soaking rice grains in water at 25°C for about one hour is required before cooking at temperatures above 70°C for 20 minutes or more. The moisture content for fully cooked rice grains can rise above 65% moisture content (wet basis).

Recently NMR techniques have been used to analyse moisture profiles for starchy materials. During the boiling of wheat grains, Stapley (1995) found fairly sharp moisture fronts which moved approximately linearly with time. This suggests possible similarities with non-Fickian diffusion of liquid solvents into polymers (Thomas and Windle, 1982). Such behaviour may be distinguished by a sharp penetrant front that moves at a constant velocity and the resulting solvent uptake rate is constant with time. However for wheat grains, the front is not a severe discontinuity in concentration since moisture also diffuses ahead of the front. This suggests that the diffusion process may be anomalous, meaning that it lies between purely Fickian and purely non-Fickian diffusion. However, the linear fronts seen in wheat grains can also be explained with a purely Fickian diffusion model for moisture uptake, if the finite resistance of the outer pericarp of the wheat is taken into account (Landman and Please, 2000). Since individual rice particles in grist have no outer pericarp and consist of pure endosperm only, this model is not appropriate here. Some NMR work has recently been undertaken for rice grains (Takeuchi et al., 1997a; Takeuchi et al., 1997b) but the conclusions are not as clear as for Stapley's wheat experiments.

Using NMR and other techniques, the moisture diffusivity has been carefully measured for wheat (Stapley, 1995) for rice starch/water mixtures (Gomi et al., 1998) and for corn kernel (Syarief et al., 1986). The diffusivity is found to be a strongly increasing function of moisture content, which can be fitted to either a power law or an exponential form. A Fickian model for water uptake gives rise to nonlinear diffusion equations inside a swelling sphere.

As water is taken up by a rice particle, the starch granules undergo a gelatinisation reaction, the term generally used to describe the swelling and hydration of the granular starch (Whistler et al., 1984). With adequate water, gelatinisation occurs if the temperature is high enough, and the swelling is irreversible. There is a minimum temperature, $T_{g\,min}$, at which gelatinisation occurs. Below this temperature starch granules swell slightly, but the swelling is reversible (Beynum, 1985). In its narrowest sense gelatinisation is the thermal disordering of crystalline structures in native starch granules (Tester and Morrison, 1990).

Gelatinisation has also been described as the bursting of granules in the presence of hot water (Kunze, 1996). A thorough liteature overview on gelatinisation is given in Stapley (1985).

The gelatinisation temperature and the amount and speed of swelling are influenced by the ratio of amylopectin to amylose, the amount of other material such as lipids and proteins as well as the initial water content and the size of the starch granules. The minimum gelatinisation temperature for rice is usually around 68-75°C although the exact temperature varies between different types of grain, and between granules of the same grain (Juliano, 1985; Lund and Wirakartakusumah, 1984). The temperature of gelatinisation increases with decreasing availability of water (Biliaderis et al., 1986; Juliano, 1985). A schematic of the experimentally derived relationship between local moisture content and gelatinisation temperature is shown in Figure 1.

Suzuki and coworkers (Suzuki et al., 1976; 1977) have studied the cooking mechanism of rice at different temperatures. By measuring the proportion of the soft rice grain at different times, the cooking rate was estimated. It was concluded that the cooking process consisted of two mechanisms. At temperatures below 110°C the cooking was limited by the gelatinisation process, but above 110°C the cooking was limited by the diffusion rate of water through the cooked layer.

Experimental work for both rice and wheat suggests that gelatinisation causes a step change in the water diffusivity of starch – the diffusivity is found to increase greatly when a grain is cooked (Stapley et al.,1998; Suzuki et al., 1977). During the process of cooking when the grain has an internal region which is uncooked and a outer region which is cooked, we deduce that the inner uncooked region will have a water diffusivity an order of magnitude smaller than the outer cooked region. This assumption allows us to employ some asymptotic approximations to solving the nonlinear diffusion model.

Cooking model

A single rice particle is considered here. A derivation of the underlying water uptake model is presented where the particle swells due to absorbtion of water. Let ϕ be the volume fraction occupied by water, while $1-\phi$ is the volume fraction of solid, assumed here to be all starch. Let the average fluid and solid velocity within a particle be $\mathbf{u}_w$ and $\mathbf{u}_s$ respectively, as defined in Bear (1972). Then the volumetric flux of water is $\phi\,\mathbf{u}_w$. Assuming the densities of water and solid are constant, the mass conservation equations are

$$\frac{\partial \phi}{\partial t} + \nabla \cdot (\phi\,\mathbf{u}_w) = 0\,, \tag{1}$$

$$\frac{\partial (1-\phi)}{\partial t} + \nabla \cdot ((1-\phi)\mathbf{u}_s) = 0\,. \tag{2}$$

These equations can be combined to produce

$$\nabla \cdot (\phi\, \mathbf{u}_w + (1-\phi)\mathbf{u}_s) = 0\,. \tag{3}$$

Assuming that all velocities are in a radial direction, this integrates to give

$$\phi\, \mathbf{u}_w + (1-\phi)\mathbf{u}_s = 0\,, \tag{4}$$

since all velocities are zero at the centre at $r = 0$.

For flow in a fixed stationary porous media Darcy's Law can be generalised to give

$$\mathbf{u} = -k\nabla\psi\,, \tag{5}$$

where $\mathbf{u}$ is the velocity of the fluid and ψ is a velocity potential (Bear, 1972). Here we assume that ψ is a function of ϕ only. For the case of flow through a moving solid, $\mathbf{u}$ in (5) is replaced by the relative velocity of the fluid $\mathbf{u}_w - \mathbf{u}_s$ to give

$$\mathbf{u}_w - \mathbf{u}_s = -k\nabla\psi\,. \tag{6}$$

The velocity $\mathbf{u}_w$ is determined using equations (4) and (6). Substitution into the conservation equation (1) then gives

$$\frac{\partial\phi}{\partial t} = \nabla \cdot \left[\phi(1-\phi)k\frac{d\psi}{d\phi}\nabla\phi\right]\,. \tag{7}$$

If we define the diffusivity as

$$D(\phi) \equiv \phi(1-\phi)k\frac{d\psi}{d\phi} \tag{8}$$

this leads to the nonlinear diffusion equation describing the water uptake

$$\frac{\partial\phi}{\partial t} = \nabla \cdot (D(\phi)\nabla\phi)\,. \tag{9}$$

Assuming that a piece of rice is spherical with radius R, it is convenient to consider a spherically symmetric geometry for the rice particle and determine the water volume fraction $\phi(r,t)$ satisfying

$$\frac{\partial\phi}{\partial t} = \frac{1}{r^2}\frac{\partial}{\partial r}\left(r^2 D(\phi)\frac{\partial\phi}{\partial r}\right)\,. \tag{10}$$

As water is absorbed, the sphere will swell giving an evolving surface radius $R = R(t)$. To generate an equation for the rate of change of $R(t)$ with time, the total mass inside the swelling sphere is determined by integrating equation (10) over the solid spherical volume as

$$\int_0^{R(t)} \frac{\partial\phi}{\partial t} r^2 dr = \int_0^{R(t)} -\frac{\partial(1-\phi)}{\partial t} r^2 dr = \int_0^{R(t)} \frac{\partial}{\partial r}\left(r^2 D(\phi)\frac{\partial\phi}{\partial r}\right) dr\,. \tag{11}$$

Using Leibniz's rule to interchange the time derivative and spatial integration, and noting that $\frac{\partial \phi}{\partial r}(0,t) = 0$, gives

$$[1 - \phi(R(t),t)]\, R^2 \frac{dR}{dt} = \frac{d}{dt}\left(\int_0^{R(t)} (1-\phi) r^2 dr \right) + R^2 D(\phi(R(t),t)) \frac{\partial \phi}{\partial r}(R(t),t)\,. \quad (12)$$

The left hand-side is proportional to the rate of change of the spherical volume. The first term on the right hand-side is proportional to the time rate of change of the total volume of solids in the rice particle. This term accounts for any possible solids loss and it is nonzero when dissolution of solids is considered in a later section. The last term represents the flux of water through the grain surface contributing to the increase in volume of the swelling sphere.

Since the inhibiting outer pericarp has been milled from the rice, the concentration at the boundary is assumed to be a constant value corresponding to equilibrium or saturation, and it is written as

$$\phi(R(t),t) = \phi_1\,. \quad (13)$$

Experimental work indicates that ϕ_1 may vary with temperature (Takeuchi et al., 1997b) for temperatures above 50°C. For fixed temperature, clearly ϕ_1 is a constant.

Rearranging (12) gives an equation for the movement of the outer boundary as

$$\frac{dR}{dt} = \left(\frac{D(\phi_1)}{1-\phi_1} \right) \frac{\partial \phi}{\partial r}(R(t),t) + \frac{1}{(1-\phi_1)R^2} \frac{d}{dt}\left(\int_0^{R(t)} (1-\phi) r^2 dr \right)\,. \quad (14)$$

In this section, we will suppose that the total mass of solid inside the swelling sphere remains constant, so that the last term in (14) is zero. Then we have a simplified evolution equation for R as

$$\frac{dR}{dt} = \frac{D(\phi_1)}{1-\phi_1}\, \frac{\partial \phi}{\partial r}(R(t),t)\,. \quad (15)$$

Here the change in the radius is due to water intake only. Note that this equation can also be derived by assuming that dR/dt is proportional to the velocity of solids at the boundary, giving a so-called kinematic condition.

We assume that the water is initially uniformly distributed inside the rice particle, so that

$$\phi(r,0) = \phi_0\,. \quad (16)$$

As discussed later, the moisture diffusivity is a strongly increasing function of moisture content and the diffusivity is much larger in gelatinised starch than ungelatinised starch. Then we can assume there is a steep moisture front between the dry/ungelatinised/uncooked and wet/gelatinised/cooked regions of a particle, and furthermore that gelatinisation occurs at this front. We denote the position of this front as $s(t)$. For a given temperature,

gelatinisation occurs at a certain moisture volume fraction denoted as ϕ_g (as illustrated in Figure 1), hence we write

$$\phi(s(t), t) = \phi_g \, . \tag{17}$$

Furthermore we assume that the diffusivity is discontinuous at $s(t)$ (Stapley et al., 1998). For simplicity we assume that no moisture diffuses ahead of the gelatinisation front which means that $D(\phi)$ is zero for $\phi < \phi_g$. Hence the ungelatinised region is at the initial moisture content $\phi(r, t) = \phi_0$ for $0 \leq r < s(t)$. The gelatinisation front is approximated by a water volume fraction discontinuity or shock at $\phi(s(t), t) = \phi_g$, namely

$$\phi(s^+, t) = \phi_g \quad , \quad \phi(s^-, t) = \phi_0 \, . \tag{18}$$

An equation for the motion of this discontinuity can be obtained by performing a mass balance across the discontinuity. Multiplying equation (10) by r^2 and integrating across the front from $r = s^-$ to $r = s^+$ gives

$$\int_{s^-}^{s^+} \frac{\partial \phi}{\partial t} r^2 dr = \int_{s^-}^{s^+} \frac{\partial}{\partial r} \left(r^2 D(\phi) \frac{\partial \phi}{\partial r} \right) dr \, . \tag{19}$$

Interchanging the time derivative and spatial integration on the left-hand side and integrating the right-hand side gives

$$\frac{d}{dt} \int_{s^-}^{s^+} \phi r^2 dr - (\phi_g - \phi_0) s^2 \frac{ds}{dt} = \left[s^2 D(\phi) \frac{\partial \phi}{\partial r}(s(t), t) \right]_{s^-}^{s^+} \, . \tag{20}$$

Using $D(\phi_0) = 0$, and letting s^+ and s^- tend towards the gelatinisation front $s(t)$ allows (20) to be rearranged as

$$\frac{ds}{dt} = -\frac{D(\phi_g)}{\phi_g - \phi_0} \frac{\partial \phi}{\partial r}(s(t), t) \, . \tag{21}$$

This is the equation describing the evolution of the gelatinisation front, which marks the boundary between cooked and uncooked portions of the rice particle.

The non-dimensional problem

The spatial variable, outer radius, gelatinisation front radius, volume fraction, time and the diffusivity function are scaled according to

$$\bar{r} = \frac{r}{l} \, , \; \bar{R} = \frac{R}{l} \, , \; \bar{s} = \frac{s}{l} \, , \; \theta = \frac{\phi - \phi_0}{\phi_1 - \phi_0} \, , \; \bar{t} = \frac{D(\phi_1)}{l^2} t \, , \; \mathcal{D}(\theta) = \frac{D(\phi)}{D(\phi_1)} \, , \tag{22}$$

where l is the initial radius of the sphere. Note that here the equilibruim moisture volume fraction can be a function of the temperature T. Clearly, for a cooking process held at a constant temperature, ϕ_1 is fixed. However, if the temperature is allowed to vary over the course of the cooking operation, the dimensionalisation used here needs to be modified and

any temperature dependence of the diffusivity must be taken into account. This will be addressed in a later section. In the treatment here it will be assumed that the temperature is held constant throughout the cooking process. Since we are modelling the water uptake and gelatinisation, that is the cooking of rice and not just soaking of rice, the chosen temperature is assumed to be above the minimum gelatinisation temperature indicated in Figure 1.

For convenience, the overbar notation will be dropped when the context is clear. In dimensionless terms, equation (10) becomes

$$\frac{\partial \theta}{\partial t} = \frac{1}{r^2}\frac{\partial}{\partial r}\left(r^2 \mathcal{D}(\theta) \frac{\partial \theta}{\partial r} \right) , \tag{23}$$

This nonlinear diffusion equation has the following boundary and initial conditions,

$$\theta(r,0) = 0 \quad , \quad \theta(R(t),t) = 1 \quad , \quad \theta(s(t),t) = \theta_g \quad , \quad R(0) = 1 \quad , \quad s(0) = 1 \, , \tag{24}$$

where θ_g is just the scaled gelatinisation moisture content

$$\theta_g = \frac{\phi_g - \phi_0}{\phi_1 - \phi_0} \, .$$

Since ϕ_g decreases with increasing temperature and ϕ_1 may increase with increasing temperature, the variable θ_g must decrease with increasing temperature.

In dimensionless terms, the equations (15) and (21) describing the evolution of the outer boundary and the gelatinisation front become

$$\frac{dR}{dt} = \alpha \frac{\partial \theta}{\partial r}(R(t),t) \, , \tag{25}$$

$$\frac{ds}{dt} = -\beta \frac{\partial \theta}{\partial r}(s(t),t) \, , \tag{26}$$

where we have introduced parameters α and β defined by

$$\alpha = \frac{\phi_1 - \phi_0}{1 - \phi_1} \quad , \quad \beta = \frac{D(\phi_g)}{D(\phi_1)} \left(\frac{\phi_1 - \phi_0}{\phi_g - \phi_0} \right) = \frac{\mathcal{D}(\theta_g)}{\theta_g} \, . \tag{27}$$

For constant temperature T, the parameters α and β are constants.

Pseudo–steady state solution for water uptake and gelatinisation

The water uptake and gelatinisation processes inside the spherical rice particle are described by the nonlinear diffusion equation (23) with two moving boundaries. In order to gain insight into the movement of the gelatinisation front into a swelling piece of rice, we choose to explore approximate analytic solutions.

For temperatures below 110°C, Suzuki et al. (1976, 1997) concluded that the rate-determining mechanism for cooking was the gelatinisation process and not the water uptake. This implies that the outer cooked region is almost at diffusive steady state, so that the moisture profile there is termed pseudo-steady or quasi-steady state, while the inner region remains at the initial moisture content. Hence, in the outer region we set $\frac{\partial\theta}{\partial t} \approx 0$. This approach has been adopted by other authors in approaching similar nonlinear problems (Landman and Please, 2000; Landman et al., 2000; McGowan and McGuinness, 1996; McGuinness et al., 1998; McGuinness et al, 2000).

In spherical coordinates, the diffusion equation (23) in pseudo–steady state reduces to

$$\frac{\partial}{\partial r}\left(r^2\mathcal{D}(\theta)\frac{\partial\theta}{\partial r}\right) = 0\,, \tag{28}$$

Integrating this implies that the moisture profiles θ satisfies the implicit relation

$$\Gamma(\theta) = \frac{A(t)}{r} + B(t)\,, \tag{29}$$

where

$$\Gamma(\theta) = \int_0^\theta \mathcal{D}(\omega)d\omega\,. \tag{30}$$

Note that Γ is the Kirchoff transformation commonly introduced in nonlinear diffusion problems (Kirchoff, 1894). After applying the moisture boundary conditions (24), we find that the moisture profile satisfies the following equation

$$\frac{\Gamma(\theta)-\Gamma(\theta_g)}{\Gamma(1)-\Gamma(\theta_g)} = \frac{\dfrac{1}{s(t)}-\dfrac{1}{r}}{\dfrac{1}{s(t)}-\dfrac{1}{R(t)}}\,. \tag{31}$$

This equation implicitly relates θ and r at some time t, given R and s.

Equations determining the time evolution of R and s are obtained by differentiating equation (31) with respect to r, and substituting into (25) and (26) to give

$$\frac{dR}{dt} = \Omega_1\frac{1}{R^2(\frac{1}{s}-\frac{1}{R})}\,, \tag{32}$$

$$\frac{ds}{dt} = -\Omega_2\frac{1}{s^2(\frac{1}{s}-\frac{1}{R})}\,, \tag{33}$$

where

$$\Omega_1 \equiv \alpha\,[\Gamma(1)-\Gamma(\theta_g)]\,, \tag{34}$$

$$\Omega_2 \equiv \frac{\Gamma(1)-\Gamma(\theta_g)}{\theta_g}\,. \tag{35}$$

At constant temperature T, Ω_1 and Ω_2 are constant.

These equations combine to give the following equation

$$\frac{dR}{ds} = -\frac{\Omega_1}{\Omega_2}\frac{s^2}{R^2} \,. \tag{36}$$

When $\frac{\Omega_1}{\Omega_2}$ is a constant, i.e. the process is held at a constant temperature, this equation integrates to give

$$R^3 + \frac{\Omega_1}{\Omega_2}s^3 = 1 + \frac{\Omega_1}{\Omega_2} \,. \tag{37}$$

Equation (37) can be rearranged to express s as an explicit function of R as

$$s \equiv S(R) = \left[\frac{\Omega_2}{\Omega_1}(1 + \frac{\Omega_1}{\Omega_2} - R^3)\right]^{\frac{1}{3}} \,. \tag{38}$$

With $S(R)$ determined, equation (32) can be integrated to obtain an expression for $R(t)$:

$$\int_1^R r^2 \left(\frac{1}{S(r)} - \frac{1}{r}\right) dr = \Omega_1 t \,. \tag{39}$$

This can be evaluated to give

$$(1 + \frac{\Omega_1}{\Omega_2}) - (R^2 + \frac{\Omega_1}{\Omega_2}S^2) = 2\Omega_1 t \,. \tag{40}$$

We now determine the gelatinisation time, that is the time when the gelatinisation front reaches the centre of the rice particle. First the radius of the sphere at this time can be found by setting $s = 0$ in (37), giving the maximum radius of the swelled rice particle as

$$R_g = \left(1 + \frac{\Omega_1}{\Omega_2}\right)^{\frac{1}{3}} \,. \tag{41}$$

This implies that when gelatinisation is complete, the volume expansion factor of a single grain, VEF, is given by

$$\text{VEF} = 1 + \frac{\Omega_1}{\Omega_2} = 1 + \alpha\theta_g \,. \tag{42}$$

The time required for the rice particle to be fully gelatinised is then determined from (40) by setting $S = 0$ and $R = R_g$ as

$$t_g = \frac{1}{2\Omega_1}\left[\left(1 + \frac{\Omega_1}{\Omega_2}\right) - \left(1 + \frac{\Omega_1}{\Omega_2}\right)^{\frac{2}{3}}\right] \,. \tag{43}$$

The above approximate solutions will only be valid for $t \leq t_g$. The steady-state assumption breaks down after the time $t = t_g$ since then the moisture at the rice centre increases above θ_g. Since our interest is in the dissolution process occurring simultaneously with the moisture uptake and gelatinisation model, there will be no need for a model for times greater than t_g.

Asymptotic solutions

Explicit expressions for R and s valid for small times can be obtained from equations (37) and (40) using asymptotic analysis. For $t \ll 1$, we obtain expansions as

$$R(t) = 1 + \Omega_1 \sqrt{\frac{2}{\Omega_1 + \Omega_2}}\ t^{\frac{1}{2}} - \frac{2\Omega_1}{3}\left(\frac{\Omega_1 + 2\Omega_2}{\Omega_1 + \Omega_2}\right) t + O(t^{\frac{3}{2}})\,, \tag{44}$$

$$s(t) = 1 - \Omega_2 \sqrt{\frac{2}{\Omega_1 + \Omega_2}}\ t^{\frac{1}{2}} - \frac{2\Omega_2}{3}\left(\frac{2\Omega_1 + \Omega_2}{\Omega_1 + \Omega_2}\right) t + O(t^{\frac{3}{2}})\,. \tag{45}$$

These expansions show that $1 - s(t)$ and $R(t) - 1$ are both proportional to $\sqrt{t}$ for small t; this square root time behaviour is expected for diffusive processes. For small t, the ratio of the speeds of the fronts is just $\dfrac{\Omega_1}{\Omega_2}$ (this also follows from (36)). The effect of the spherical geometry and curvature is accounted for by the $o(\sqrt{t})$ terms, which leads to an increase in the gelatinisation front speed as it approaches the centre.

Asymptotic analysis can also be performed near the end of the gelatinisation process, that is for times near t_g. The following expressions are valid for $t_g - t \ll 1$:

$$R(t) \;=\; R(t_g) - \frac{2\Omega_1\sqrt{2\Omega_2}}{3(1 + \frac{\Omega_1}{\Omega_2})^{\frac{2}{3}}}(t_g - t)^{\frac{3}{2}} - O((t_g - t)^2)\,, \tag{46}$$

$$s(t) \;=\; \sqrt{2\Omega_2}(t_g - t)^{\frac{1}{2}} + O(t_g - t)\,. \tag{47}$$

Numerical solutions

In this section, we numerically determine the locations of $s(t)$ and $R(t)$ by solving the system of differential equations (32)-(33) and discuss their dependence on the dimensionless gelatinisation moisture fraction θ_g. We first choose an appropriate diffusivity function at fixed temperature with exponential form as

$$D(\phi) = Ae^{c\phi}\,, \tag{48}$$

where A and c are experimentally determined constants. With this choice the corresponding function $\Gamma(\theta)$ is

$$\Gamma(\theta) = \frac{1}{\nu}(e^{\nu(\theta-1)} - e^{-\nu})\,, \tag{49}$$

where

$$\nu = c(\phi_1 - \phi_0)\,. \tag{50}$$

Note that R and s will now depend on the values of ν and θ_g.

Diffusivity measurements for ground rice starch/water mixtures are reported by Gomi et al. (1998). These estimates are expected to be larger than those for whole rice grains. The measurements were fitted to a sum of exponential functions over a wide range of the wet basis moisture contents. In terms of the volume fraction ϕ, these can be fitted just as well by the simple exponential form (48) as

$$D(\phi) = 1.43 \cdot 10^{-7} e^{5.22\phi} \quad \mathrm{cm}^2/\mathrm{s} \text{ at } 25^\circ\mathrm{C}\,.$$

Without further data, we choose $c = 5.22$ here. The value of $D(\phi_1) = Ae^{c\phi_1}$ is needed for the time scaling; this quantity is expected to be substantially smaller than the value calculated from Gomi's numbers. However, the accurate determination of diffusivity and its dependence on moisture content is still needed for whole grain milled rice before the results in this paper can be confidently quantified. As discussed earlier, the equilibruim moisture volume fraction ϕ_1 may vary for temperatures above 60°C. Data for this is inconclusive, although it is agreed that in boiling or close to boiling situations, the wet basis moisture content is approximately 0.73 (Juliano, 1985; Ramesh and Rao, 1996) This converts to a moisture volume fraction of approximately 0.8. In general, we might expect ϕ_1 to decrease from this value as temperature decreases.

As noted earlier, as temperature decreases $\theta_g(T)$ increases. Using the parameter values in Table 1a for our calculations, typical values of Ω_1 and Ω_2 can be obtained, as shown in Table 1b. Note that the parameters Ω_1 and Ω_2 decrease with increasing θ_g, whereas the ratio $\frac{\Omega_1}{\Omega_2}$ increases with increasing θ_g.

The positions of $R(t)$ and $s(t)$ for different values of θ_g are illustrated in Figures 2 and 3. These figures are qualitatively the same as the results of McGuinness et al. (1998, 2000). If more water absorbtion is required for gelatinisation, the time required will increase, so that t_g increases with increasing θ_g. This in turn gives an increase in the amount of swelling. Note that in the limit as $\theta_g \to 1$, the rice particle comes to equilibrium moisture content (in infinite time) and the VEF $\to 4$ for this choice of parameter values. This is the approximate value obtained experimentally by Ramesh and Rao (1996).

Figures 2 and 3 also illustrate the correct asymptotic form in the small t and small $t_g - t$ limits, as given in the previous subsection.

Dissolution of starch molecules

The main goal of the cooking process under investigation is to free starch molecules from the grist, allowing enzymes to break these large molecules into small molecular weight

sugars. After the starch granules have been gelatinised, the starch molecules must escape from the ruptured granule within the whole rice particle and dissolve into the bulk solution.

The process of dissolution is of little concern when using flours instead of whole rice grains or grist, because the flour particle sizes are much smaller and hence (provided there is no agglomeration taking place) dissolution occurs very rapidly. For this reason, many texts on brewing ignore the dissolution process and just cover gelatinisation followed directly by liquefaction and saccharification (Kunze, 1996).

In this section the factors determining and influencing the rate of dissolution of rice grist will be discussed including the differences between polymeric and non-polymeric species. Two models for dissolution are proposed and explored – the first being a discrete model and the second a continuous model. Both of these incorporate and build on the moisture uptake and gelatinisation model described in the previous section. The two dissolution models are compared and shown to give equivalent results when parameters are matched in a natural way.

Background to the model

For low molecular weight non-polymeric species, the dissolution rate is predominantly governed by the mass transfer resistance (Devotta et al., 1994a; Ranade and Mashelkar, 1995). The overall rate of mass transfer is indirectly a function of the particle size, through being a function of exposed surface area. If a particle is cut in half then it has more exposed surface, and so dissolution can occur from this new surface. This is also true for water uptake rates, as can be seen in the time nondimensionalisation in equation (22).

For high molecular weight polymers, the dissolution process is much more complicated, because the long chains must first disentangle themselves before they are able to dissolve in solution.

A reptation model for the behaviour of entangled polymers has been developed by (de Gennes, 1979), and applied to the dissolution of polymers (Herman and Edwards, 1998; Papanu et al., 1989). One of the key elements of this model is that a polymer chain requires a certain amount of time, called the reptation time, to become disentangled from a polymer network. After solvent uptake by the polymer network, dissolution will begin only after the reptation time. As a consequence there is a critical particle size, below which the dissolution time is no longer dependent on the size of the particle (Devotta et al., 1994a; Ranade and Mashelkar, 1995). Devotta et al., (1994a) obtained the first experimental results that showed the existence of a critical particle size. This is in marked contrast to the dissolution of non-polymeric low molecular weight compounds, where a smaller particle size leads to a faster dissolution rate.

There are additional factors influencing the rate of dissolution of starch. Amylose and

amylopectin, the two types of starch polymers, behave differently after gelatinisation has occurred, because of their different structure and size. A limitation of the reptation-based dissolution models is that they are valid only for linear polymer chains, hence they cannot be applied to the highly branched amylopectin starch.

One of the implications of this theory is that if the mass transfer rate is higher than the reptation rate, then the dissolution process will be limited by the rate of reptation. On the other hand if mass transfer is slower and therefore rate limiting, then reptation will not be as important (Papanu et al., 1989).

There is evidence during the industrial rice cooking process that mechanical stirring promotes rapid rates of dissolution. One explanation of this effect is that once the starch granules are gelatinised and ruptured the starch polymers are sheared away from the surface and consequently the starch at the boundary of the rice particle will quickly dissolve into the liquid solution. This is equivalent to the assumption that the dissolution time scale (or reptation time) is much smaller than the gelatinisation time scale. The action of enzyme on the surface of the particle will also promote rapid dissolution. (In a later section, we will add more complexity to this model by addressing the changing composition of the surrounding solution as the starch dissolves.)

With these assumptions, we develop a discrete model and a continuous model for the dissolution process. The two models are then made equivalent.

Discrete dissolution model

For the discrete dissolution model, the rice particle interior is taken to consist of concentric spherical shells of starch granules. The entire spherical shell of starch granules at the boundary, once ruptured by gelatinisation, is assumed to immediately peel away from the rice particle.

Let Δ be a measure of the size of a starch granule, scaled by the initial radius of the sphere, so that $l\Delta$ represents the real physical granule size. We assume that a shell of starch granules is removed from the particle once all the granules in the shell are gelatinised. Hence the region between R and s is removed and goes into solution. These shells will be removed one at a time, as the gelatinisation front progresses into the rice particle.

The steps describing this process are as follows. We start with a rice particle with $R(0) = s(0) = 1$, and $\theta(r, 0) = 0$, for $0 \leq r < 1$. Using the gelatinisation and water uptake model described in a previous section, water is absorbed into the rice particle and it swells a certain amount. We define a time T_p, when $s(T_p) = 1 - \Delta$. At this time, the shell of swelled material between R and s is removed from the particle and goes into solution. Hence at this time, R is reset to $s(T_p)$. Thereafter the rice particle again swells with water uptake, and the gelatinisation model is now solved with new initial conditions

$R = s = 1 - \Delta$. When $s = 1 - 2\Delta$ the next shell peels away. This cycle of gelatinisation and removal continues until $s = 0$.

Starting with a sphere of unit radius with initial conditions $R(0) = s(0) = 1$, we have defined a time T_p, when the first shell is removed, as

$$s_p = s(T_p) = 1 - \Delta \,. \tag{51}$$

The gelatinisation model gives a relationship between R and s given by (37). Hence the position of the outer boundary at the peeling time can be determined as

$$R_p = R(T_p) = \left[(1 + \frac{\Omega_1}{\Omega_2}) - \frac{\Omega_1}{\Omega_2}(1 - \Delta)^3 \right]^{\frac{1}{3}} \,. \tag{52}$$

These values of s_p and R_p allow us to write the peeling time, using equation (40), as

$$T_p(\Delta) = \frac{1}{2\Omega_1} \left[1 + \frac{\Omega_1}{\Omega_2} - \left[(1 + \frac{\Omega_1}{\Omega_2}) - \frac{\Omega_1}{\Omega_2}(1 - \Delta)^3 \right]^{\frac{2}{3}} - \frac{\Omega_1}{\Omega_2}(1 - \Delta)^2 \right] \,. \tag{53}$$

For thin shells ($\Delta \ll 1$), a Taylor series expansion of $T_p(\Delta)$ in terms of Δ gives

$$T_p(\Delta) = \Delta^2 \left[\left(\frac{\Omega_1 + \Omega_2}{2\Omega_2^2} \right) - O(\Delta) \right] \,. \tag{54}$$

Since the first term in the series is $O(\Delta^2)$, when Δ is doubled then T_p increases by a factor of four. (This first term can also be obtained from the asymptotic expression (45).)

The time to peel off one layer from a dimensionless sphere of unit radius is given by equation (53). To generalise this to a sphere of dimensionless radius r ($0 < r < 1$), the scalings of length and time are taken into account as given in (22). The peeling time for a sphere of radius r is r^2 multiplied by the peeling time for a sphere of radius unity. The physical peeling depth $l\Delta$ remains constant. The scaled peeling depth is obtained by dividing the physical peeling depth by the physical radius of the sphere lr, giving the value Δ/r.

The peeling time T_{pr} for a piece of grist of dimensionless radius r is then given in terms of T_p as

$$T_{pr}(r, \Delta) = r^2 \, T_p(\frac{\Delta}{r}) \,. \tag{55}$$

Note that

$$T_{pr}(1, \Delta) = T_p(\Delta) \,. \tag{56}$$

Using the expansion (54) we find that

$$T_{pr}(r, \Delta) = r^2 \, T_p(\frac{\Delta}{r}) = \Delta^2 \left[\left(\frac{\Omega_1 + \Omega_2}{2\Omega_2^2} \right) - \frac{1}{r} O(\Delta) \right] \,. \tag{57}$$

This shows that the radius of the sphere does not affect the peeling time when $r \gg \Delta$. Comparing equations (54) and (57) we observe that if $r < 1$ then $T_{pr} < T_p$, and

$$T_{pr}(r, \Delta) = T_p(\Delta) \left[1 - \left(\frac{1}{r} - 1 \right) O(\Delta) \right] . \tag{58}$$

Therefore if $\Delta \ll r$ we have

$$T_{pr}(r, \Delta) \approx T_p(\Delta) . \tag{59}$$

Evaluating T_{pr} as a function of r, as plotted in Figure 4, shows that this approximation is in fact valid for a large range of r values.

The total time for dissolution T_d can now be determined by summing the peeling times for each layer as $s \to 0$ in steps of Δ. Since the physical size of a rice particle is l, and the physical size of a layer is $l\Delta$, the number of layers to be peeled off is $1/\Delta$. Without much loss of accuracy for small Δ, we assume that $1/\Delta$ is an integer. The nondimensional radius after each layer is peeled off will be a multiple of Δ ie. $r = i\Delta$ where $i = 1, 2, ...1/\Delta$. The total dissolution time T_d is then given by the sum

$$T_d = \sum_{i=1}^{1/\Delta} T_{pr}(i\Delta, \Delta) . \tag{60}$$

This expression may be approximated by a simpler expression using (59). An approximate dissolution time (which is also an upper bound on the actual dissolution time) is given by

$$T_d \approx \frac{T_p(\Delta)}{\Delta} . \tag{61}$$

To demonstrate this graphically, in the limit as $\Delta \to 0$, the sum in (60) can be replaced by an integral, giving

$$T_d \approx \frac{1}{\Delta} \int_0^1 T_{pr}(r, \Delta) dr .$$

Since this integral represents the area under the curve in Figure 4 and the curve is well approximated by a constant when Δ is sufficiently small, the approximation (61) follows.

The time T_d can be further simplified using the expansion (54), giving

$$T_d \approx \left(\frac{\Omega_1 + \Omega_2}{2\Omega_2^2} \right) \Delta + O(\Delta^2) . \tag{62}$$

Consequently, for thin shell layers the dissolution time is proportional to the shell thickness Δ, that is, the dissolution time is linear in Δ.

An approximate velocity for the gelatinisation front can be calculated for this model. For a sphere of radius r, the front travels a distance Δ from the surface in the peeling time $T_{pr}(r, \Delta)$. This gives an estimate of the average velocity for each step as

$$\frac{\Delta}{T_{pr}(r, \Delta)} . \tag{63}$$

Alternatively, over the entire dissolution process for a sphere with dimensionless radius of unity, the average velocity is $1/T_d$. Using the approximation for T_d from equation (61) this velocity is

$$v_{av} = \frac{1}{T_d} \approx \frac{\Delta}{T_p(\Delta)} \approx \left(\frac{2\Omega_2^2}{\Omega_1 + \Omega_2} \right) \frac{1}{\Delta} \,, \tag{64}$$

Consistent with our previous arguments, the average velocity over the whole process is well approximated by the average velocity of the first peeling step.

Continuous dissolution model

We return to examining more closely the conservation of mass equation (14), which describes the velocity of the outer boundary. The last term is proportional to the rate of change of the solids volume. When the rice is undergoing dissolution, this term will be negative. The first term on the right hand side represents the flux of water into the particle which causes the particle to swell. Hence these two opposing effects contribute to the growth rate of R with time; that is $\frac{dR}{dt}$ equals the difference between swelling rate and the dissolution rate.

Taking into account the dissolution term in (14) and non-dimensionalising in the same way as previously, the evolution equations for the two fronts R and s (32)- (33) are modified to become

$$\frac{dR}{dt} = \Omega_1 \frac{1}{R^2(\frac{1}{s} - \frac{1}{R})} - \lambda \tag{65}$$

$$\frac{ds}{dt} = -\Omega_2 \frac{1}{s^2(\frac{1}{s} - \frac{1}{R})} \,. \tag{66}$$

Here we have introduced a term λ which represents the dimensionless solid dissolution rate:

$$\lambda(t) = -\frac{1}{(1-\phi_1)R^2} \frac{d}{dt} \left(\int_0^{R(t)} (1-\phi) r^2 dr \right) \,, \tag{67}$$

Now the position $R(t)$ represents the location of the outer boundary and dissolution front. These equations will only be valid for times until the gelatinisation front reaches the centre of the rice particle. A similar treatment is used for the dissolution of polymers (Devotta et al., 1994a, 1994b; Papanu et al., 1989).

Consider the case λ is constant. As discussed earlier, given that dissolution occurs rapidly compared to gelatinisation, the dissolution front R is expected to be close to the gelatinisation front s. Therefore dissolution will be almost complete when $s(t) = 0$, and the system equations (65) - (66) can be used to give an approximation for the dissolution time.

Set $R = s + \delta_p$, so that δ_p represents the thickness of the region between the gelatinisation front and the dissolution front; it is expected to be small. Then equations (65) and (66) can be rewritten as

$$\frac{dR}{dt} = \frac{\Omega_1}{\delta_p}\frac{s}{R} - \lambda \tag{68}$$

$$\frac{ds}{dt} = -\frac{\Omega_2}{\delta_p}\frac{R}{s}\,. \tag{69}$$

Since $R(0) - s(0) = \delta_p(0) = 0$, initially and for early times $\frac{dR}{dt} > 0$ and $\frac{ds}{dt} < 0$. Hence $\frac{d(R-s)}{dt} > 0$ so that the thickness of the gelatinised shell $R(t) - s(t)$ increases. Provided $\delta_p \ll s$, δ_p reaches the following asymptotic size

$$\delta_p \sim \frac{\Omega_1 + \Omega_2}{\lambda}\,. \tag{70}$$

When s is order one, $\delta_p \ll s$ requires that

$$\lambda \gg \Omega_1 + \Omega_2 \tag{71}$$

When the shell thickness reaches the asymptotic size (70), this relation may be used to eliminate λ. Then the two differential equations are the same, so that $\frac{dR}{dt} \approx \frac{ds}{dt} \approx -\frac{\Omega_2}{\delta_p}$. Hence in this regime the shell thickness is almost constant with approximate thickness $\frac{\Omega_1+\Omega_2}{\lambda}$. At later times, s accelerates towards zero. For larger values of the parameter λ, the approximations of constant $R - s$ and hence constant $\frac{dR}{dt}$ and $\frac{ds}{dt}$ remain valid for a larger proportion of the process. Hence for a given λ, the approximate thickness of the gelatinised region is given by (70).

Under this requirement, an estimate of the speed of the dissolution front v_d can be determined using the approximations

$$v_d \approx -\frac{dR}{dt} \approx \frac{\Omega_2}{\delta_p} = \frac{\lambda}{1 + \dfrac{\Omega_1}{\Omega_2}}\,. \tag{72}$$

In dimensionless terms, since the front travels a unit distance, the dissolution time t_d is well approximated by $1/v_d$,

$$t_d = \frac{1}{\lambda}\left(1 + \frac{\Omega_1}{\Omega_2}\right)\,. \tag{73}$$

We now investigate numerical solutions to the continuous model (65) - (66), and discuss the validity of the approximations. The parameter values used are given in Table 1a with $\theta_g = 0.6$. With $\lambda \geq 10$ the requirement (71) is certainly satisfied.

Figure 5 shows that R and s are almost linear with time over their full range and that the thickness of the gelatinised region $R - s$ is approximately constant as predicted by

the analysis above. For smaller values of δ_p, the approximation for the dissolution time is very good; for example, with $\lambda = 50$ the numerical solution gives $R = 0$ at a time equal to 0.051, whereas the approximation (73) for the dissolution time gives 0.056. (For these figures, for a short time period after $s = 0$, the equation for R has been approximated by $\frac{dR}{dt} = -\lambda$.)

It is worth noting that if (71) is not satisfied then $R(t)$ is almost linear with time whereas $s(t)$ has a similar shape to that in the gelatinisation model illustrated in Figure 2.

In practice if the choice of parameters satisfies the condition (71), we find that the constant thickness approximation dominates over most of the dissolution process. Our results illustrated in Figure 5 are similar to the numerical and experimental results of Peppas et al (1994). Their figures also show constant front speeds with a gel region of constant thickness. The short time behaviour of their numerical results is different from ours due to their particular disentanglement model for dissolution. In their model initially there is no dissolution thus giving rise to more swelling; this is followed by a sudden change in direction of the outer surface when dissolution commences. Their experimental results show a change in direction of the polymer surface which is less sudden then the predictions of their model. The long time behaviour of the graphs here and in Peppas et al. are different because of the difference in geometry. The polymer dissolution model of Edwards and Cohen (1995) which incorporates non-Fickian diffusion also gives constant front speeds.

Equivalence of the two dissolution models

The discrete and continuous models presented in the previous two sections assume that dissolution is fast compared with gelatinisation. They both give constant front speeds over most of the process time. Here the speeds of the dissolution fronts for the two models are compared and an expression for the effective dissolution rate for the discrete model is determined and compared with λ from the continuous model.

To calculate an approximate dissolution rate for the discrete model, the amount of swelling is determined. From equation (52), the position of the outer boundary at time T_p is

$$R_p = R(T_p) = \left[(1 + \frac{\Omega_1}{\Omega_2}) - \frac{\Omega_1}{\Omega_2}(1 - \Delta)^3\right]^{\frac{1}{3}} \tag{74}$$

For $\Delta \ll 1$ we obtain

$$R_p = 1 + \frac{\Omega_1}{\Omega_2}\Delta + O(\Delta^2)\,. \tag{75}$$

(The same result is obtained if the early time asymptotic results in (44) are considered together with $s \sim 1 - \Delta$.) Therefore as s reduces by Δ, R increases by $\frac{\Omega_1}{\Omega_2}\Delta$ (correct to

first order in Δ). This implies that the thickness removed after swelling is

$$R_p - s_p = \Delta \left(1 + \frac{\Omega_1}{\Omega_2}\right) + O(\Delta^2) \,. \tag{76}$$

Therefore before each layer is removed, $\left(1 + \frac{\Omega_1}{\Omega_2}\right)$ is the factor by which each layer swells.

To calculate an average rate of removal we divide $R_p - s_p$ by $T_p(\Delta)$, using its asymptotic expansion (54), and obtain

$$\frac{R_p - s_p}{T_p} = \frac{2\Omega_2}{\Delta} + O(1) \,. \tag{77}$$

Then the continuous and the discrete dissolution models give the same rate of dissolution if, to leading order,

$$\frac{2\Omega_2}{\Delta} = \lambda = \frac{\Omega_1 + \Omega_2}{\delta_p} \,. \tag{78}$$

This equation serves to relate the continuous and the discrete models, and (since $l\Delta$ is a physical starch granule size) it may be regarded as providing a physical meaning for the continuous dissolution rate λ.

Note that the same result is obtained if the average speed of dissolution of the discrete model, given by (64), is equated to the speed of dissolution of the continuous model, given by (72). Notice that the ratio of the dissolution rate and the dissolution front speed, i.e. $\frac{\lambda}{v_d}$ equals $\left(1 + \frac{\Omega_1}{\Omega_2}\right)$; this factor accounts for the swelling of the spherical particle. For the dissolution front and the gelatinisation front to move at the same rate, the dissolution rate has to be larger than the speed of the gelatinisation front to counter the effect of swelling.

Rearrangement of (78) gives an expression for the thickness of a swollen gelatinised layer in the continuous model, δ_p, in terms of the discrete unswollen peeling thickness Δ:

$$\delta_p = \left(1 + \frac{\Omega_1}{\Omega_2}\right) \frac{\Delta}{2} \,. \tag{79}$$

This relationship is now interpreted geometrically with the help of Figure 6. During one peeling event, the outer grain radius R_d and the gelatinisation front s_d for the discrete model are represented by the heavy curves. The straight line joining A to B represents the gelatinisation front travelling at the average gelatinisation velocity for the discrete model. This is required to match the actual gelatinisation front position for the continuous model, which we call $s(t)$. Because of the $\sqrt{t}$ behaviour of s_d, the slope of the line joining AB matches the slope of the curve s_d at point C located a distance $\Delta/2$ below the point A. Hence the vertical distance CD represents the half-granule thickness $\Delta/2$ multiplied by the swelling factor $\left(1 + \frac{\Omega_1}{\Omega_2}\right)$. We identify this with the length δ_p. This is the (fixed) gelatinisation thickness for the continuous model. Therefore, for the continuous model the outer radius $R(t)$ is obtained by translating the line $s(t)$ vertically upwards by the distance δ_p, as seen in Figure 6 (the distance AE = BF = δ_p).

Comparison with no-dissolution model

In the previous section a gelatinisation model in the absence of dissolution was developed; this is now referred to as the no-dissolution model. This model has now been extended to include the effects of dissolution and this is referred to as the dissolution model.

The positions of the gelatinisation front $s(t)$ obtained from the no-dissolution and dissolution model are compared in Figure 7. In the absence of dissolution, the gelatinisation front is initially proportional to $\sqrt{t}$ and it accelerates as it approaches the particle centre. Adding a constant dissolution rate to this model, where the relationship between the dissolution and gelatinisation parameters satisfies the requirement (71), leads to a faster gelatinisation front that moves at a constant rate. As the dissolution rate increases, or the effective Δ decreases, the process becomes increasingly rapid.

The effects of temperature changes

It is usual for the temperature of the rice cooker to vary over the time span of the process, hence $T = T(t)$. In this section we investigate the effect this varying temperature has on our models. The temperature can affect the process in three ways, namely, through the functional dependence of the diffusivity $D(\phi, T)$ and through the gelatinisation and saturation equilibrium moisture contents $\phi_g(T)$ and $\phi_1(T)$ respectively.

Allowing for a temperature dependence in the saturation equilibrium moisture volume fraction means that we can longer scale the variables with $\phi_1(T)$ and transform the partial differential equations to the same simple type. We introduce a fixed reference moisture volume fraction ϕ_{ref} and now scale all variables with with respect to this as

$$\theta = \frac{\phi - \phi_0}{\phi_{ref} - \phi_0} \ , \ \bar{t} = \frac{D(\phi_{ref}, T(0))}{l^2} t \ , \ \mathcal{D}(\theta, T) = \frac{D(\phi, T)}{D(\phi_{ref}, T(0))} \ . \tag{80}$$

The dimensionless equation again takes the form of a nonlinear diffusion problem (23), but now the boundary conditions are in terms of two new functions as

$$\theta(R(t), t) = \frac{\phi_1(T) - \phi_0}{\phi_{ref} - \phi_0} \equiv \theta_s(T) \quad , \quad \theta(s(t), t) = \frac{\phi_g(T) - \phi_0}{\phi_{ref} - \phi_0} \equiv \theta_g(T) \quad . \tag{81}$$

Assuming again that the diffusivity increases exponentially with concentration and taking the usual Arrhenius dependence on temperature, the diffusivity as a function of temperature and moisture content can be expressed as (McGuinness et al.,1998; Stapley, 1995)

$$D(\phi, T) = A e^{-\mathcal{E}_a/(RT)} e^{c\,\phi} \, , \tag{82}$$

where R is the universal gas constant and $\mathcal{E}_a$ is an activation energy. The modified scaled diffusivity function has the form

$$\mathcal{D}(\theta, T) = D^*(T) e^{\nu^*(\theta - 1)} \tag{83}$$

where we define

$$D^*(T) = e^{-\frac{\mathcal{E}_a}{R}\left(\frac{1}{T}-\frac{1}{T(0)}\right)} , \quad \nu^* = c(\phi_{ref} - \phi_0) . \tag{84}$$

The integrated diffusivity function Γ now varies with temperature as well and becomes

$$\Gamma(\theta, T) = \frac{D^*(T)}{\nu^*}(e^{\nu^*(\theta-1)} - e^{-\nu^*}) . \tag{85}$$

Note that for a time dependent temperature $T(t)$, the functions $D^*(T)$ and $\Gamma(\theta, T)$ are also implicitly functions of time.

Various equations and parameters from previous sections must be modified to account for a time-dependent temperature. Equations (32) - (33) determining the time evolution of R and s for gelatinisation remain valid, but now the parameters Ω_1 and Ω_2 will vary with temperature, as

$$\Omega_1(T) = \alpha \left[\Gamma(\theta_s, T) - \Gamma(\theta_g(T), T)\right] , \tag{86}$$

$$\Omega_2(T) = \frac{\Gamma(\theta_s, T) - \Gamma(\theta_g(T), T)}{\theta_g(T)} . \tag{87}$$

For the discrete model the average velocity of the dissolution front v_{av} is modified to become

$$v_{av} = \frac{2\Omega_2^2}{\Omega_1 + \Omega_2}\frac{1}{\Delta} = \frac{2\left[\Gamma(\theta_s, T) - \Gamma(\theta_g(T), T)\right]}{\theta_g(T)(\alpha\theta_g(T) + 1)}\frac{1}{\Delta} , \tag{88}$$

and for the continuous model the instantaneous dissolution velocity v_d becomes

$$v_d = \frac{\Omega_2}{\delta_p} = \frac{\lambda\Omega_2}{\Omega_1 + \Omega_2} = \frac{\lambda}{\alpha\theta_g(T) + 1} . \tag{89}$$

As carried out previously, these velocities may be matched by an appropriate identification of parameters (eg equation (78)).

Finally an approximation for the distance traveled by the dissolution front in time t can be calculated using the expression

$$\int_0^t v(T(\tau))d\tau , \tag{90}$$

where v is identified with either v_{av} or v_d.

Total dissolved solids

Two models for the gelatinisation and subsequent dissolution of the material have been developed here. These models allow for the estimation of the mass of starch molecules dissolved in solution as the cooking proceeds.

Using the realistic approximation that the solids are composed entirely of starch, an expression describing the total volume of solids dissolved will be examined, first for the case that all grains in the grist have the same size and then for an arbitary distribution of grist sizes.

For a single grain size

In dimensionless terms, the solids volume in a single spherical rice particle at time t is

$$V_s(t) = 4\pi \int_0^{R(t)} (1-\phi) r^2 dr \,, \tag{91}$$

which converts into a dimensioned solids mass of $M_s(t) = l^3 \rho_s V_s(t)$. The dimensionless solids volume which has been removed from the particle and therefore dissolved is

$$V_d(t) = V_s(0) - V_s(t) = \frac{4\pi(1-\phi_0)}{3} - V_s(t) \,. \tag{92}$$

However, in order to determine the solids volume $V_d(t)$ using (91), the moisture content ϕ (or θ) must be determined. This must be calculated numerically, with either the full nonlinear diffusion equations or through the pseudo-steady state approximations (valid for $t \leq t_g$).

Alternatives to this approach are appropriate for both types of dissolution models developed here. For the continuous model the dissolved solids volume can be obtained by differentiating (92) with respect to t and recalling the definition of the dissolution rate λ from equation (67). This manipulation gives

$$\frac{dV_d}{dt} = 4\pi\lambda(1-\phi_1) R^2(t) \,. \tag{93}$$

Equation (93) shows that the rate of increase of total dissolved solids is proportional to R^2. For a constant dissolution rate λ, this means the rate of increase of dissolved solids volume decreases as the surface area of the particles decreases. Therefore continuing the dissolution process becomes less worthwhile as time progresses. As equation (93) is based on the conservation of mass, this conclusion is valid for any dissolution model.

Integrating (93) gives

$$V_d(t) = V_s(0) - V_s(t) = 4\pi(1-\phi_1) \int_0^t \lambda \, R^2(\tau) d\tau \,. \tag{94}$$

In order to generalise the result to cases where the dissolution rate can vary with time, the λ term is left inside the integral. The advantage of this formulation is that only λ and

$R(t)$ are required to be known, whereas equation (91) requires that the moisture content throughout the rice particle be determined.

An even simpler way of calculating the amount of solid removed is obtained using the discrete model for dissolution, where shells of gelatinised solid are removed at particular times. Immediately after a shell has peeled $R(t) = s(t)$ and the particle contains only the initial uniform moisture content, so that the amount of solid remaining is therefore

$$V_s(t) = \frac{4\pi}{3}(1 - \phi_0)R^3(t) \, . \tag{95}$$

Using equation (92) the amount of solids dissolved is

$$V_d(t) = \frac{4\pi}{3}(1 - \phi_0)\left[1 - R^3(t)\right] \, , \tag{96}$$

at exactly the discrete peeling times. Hence no knowledge of ϕ in the gelatinised layer is required; only information about $R(t)$ is needed. This argument works equally well for the continuous model when the gelatinised thickness $R(t) - s(t)$ is assumed to be small compared to unity. For this case only a thin gelatinised layer holds moisture above the level ϕ_0 and the approximations above are sufficiently accurate.

Since the approximation (96) is good for both the discrete and continuous model and it is the easiest to calculate, it will be used in the following to calculate the volume of dissolved solids. If the velocity of $R(t)$ is $v(t)$ then

$$R(t) = 1 - \int_0^t v(\tau)d\tau \, . \tag{97}$$

The velocity is time dependent when the process temperature is not fixed. Using (97), equation (96) can be rewritten as

$$V_d(t) = \frac{4\pi}{3}(1 - \phi_0)\left[1 - \left(1 - \int_0^t v(\tau)d\tau\right)^3\right] \, . \tag{98}$$

Clearly, when $\int_0^t v(\tau)d\tau = 1$, dissolution is complete and $V_d(t)$ will remain constant after this time.

For a distribution of grain sizes

The total dissolved solids for a single rice particle of unit radius is given by equation (98). From this, an expression for the total dissolved solids for an arbitrary distribution of grain sizes can be derived.

Consider a sphere of initial (dimensionless) radius η. For times t such that $\int_0^t v(\tau)d\tau \geq \eta$ dissolution is complete and the dissolved solids volume will remain constant. We modify equation (98) to give the volume of dissolved solids over time as

$$V_d(\eta, t) = \frac{4\pi}{3}(1-\phi_0)\begin{cases} \eta^3 - \left(\eta - \int_0^t v(\tau)d\tau\right)^3 & \text{if } \int_0^t v(\tau)d\tau < \eta \\ \eta^3 & \text{if } \int_0^t v(\tau)d\tau \geq \eta \end{cases} \tag{99}$$

To account for a distribution of particle sizes we introduce a distribution function $p(x)$. The integral $\int_a^b p(x)dx$ represents the proportion of the number of spheres which have a radius between a and b and summing all the proportions gives $\displaystyle\int_0^\infty p(x)dx = 1$. Using the scalings we have introduced, the total mass of uncooked rice is $\frac{4\pi}{3}\rho\, l^3 \displaystyle\int_0^\infty x^3 p(x)dx$ where ρ is the average density of uncooked rice. For a discrete distribution of grist of unit radius, we use $p(x) = \delta(1-x)$ where δ is the Dirac delta function.

The total volume of dissolved solids from a distribution of particle sizes as a function of time can then be expressed as

$$\begin{aligned} V_{td}(t) &= \int_0^\infty p(x)V_d(x,t)dx \\ &= \frac{4\pi(1-\phi_0)}{3}\int_0^{\int_0^t v(\tau)d\tau} x^3 p(x)dx \\ &\quad -\frac{4\pi(1-\phi_0)}{3}\int_{\int_0^t v(\tau)d\tau}^\infty \left[x^3 - (x - \int_0^t v(\tau)d\tau)^3\right] p(x)dx\,. \end{aligned} \tag{100}$$

Dissolution rate varying with solution concentration

In the previous analyses, we have assumed that the dissolution rate is a constant. In this section, we are interested in estimating the amount of water that needs to be added to the rice grist to achieve full dissolution. This requires that we consider the effect of an increasing concentration of dissolved solids in the surrounding solution on the dissolution rate λ.

Hence we allow the dissolution rate to vary with time. Suppose that λ is proportional to some power of the difference between the liquid concentration in solution and the liquid concentration at the grist outer surface, namely

$$\lambda(t) = k\left(\frac{\phi_{sol}(t) - \phi_1}{1-\phi_1}\right)^n, \tag{101}$$

where k and n are constants ($n > 0$).

It is now possible that the dissolution rate goes to zero before all of the available starch has dissolved. This will manifest itself as a minimum water-to-rice ratio. Hence, we are seeking the possibility that $\phi_{sol}(t) = \phi_1$ before all of the grist has dissolved.

Let W be the initial volume of water added per unit volume of raw rice and let V_r be the initial volume of the raw rice. To calculate $\phi_{sol}(t)$ we need to take account of the water already in the uncooked raw rice, since this will also be released into solution as the starch dissolves. The total volume of dissolved solids is $V_{td}(t)$; hence the initial moisture locked inside the raw grist which is also released with the solids is just $\frac{\phi_0 V_{td}(t)}{1-\phi_0}$. (We have assumed that all the gelatinised rice is dissolved and hence the only water inside the rice is the water that was initially there.) The volume fraction of water in the solution is the ratio of the volume of water to the total volume (dissolved solids plus water):

$$\phi_{sol}(t) = \frac{WV_r + \dfrac{\phi_0}{1-\phi_0} V_{td}(t)}{WV_r + \dfrac{V_{td}(t)}{1-\phi_0}} \,. \tag{102}$$

The dissolution process will be incomplete if $\phi_{sol}(t) = \phi_1$ before all the grist has had time to dissolve. This defines a possible non-maximum value V_f for dissolved solids volume at the time when dissolution comes to an end. Since $(1-\phi_0)V_r$ is the initial total solids volume available, we can rewrite equation (102) as

$$\frac{V_f}{(1-\phi_0)V_r} = \min\left[W\frac{(1-\phi_1)}{(\phi_1-\phi_0)}, 1 \right] \,. \tag{103}$$

Consequently, dissolution is incomplete when

$$W < \frac{\phi_1 - \phi_0}{1-\phi_1} \,. \tag{104}$$

(Note that this upper bound is just α defined in (27).) Hence for values of W satisfying this constraint, the dissolution does not proceed to completion. Alternatively, if

$$W \geq \frac{\phi_1 - \phi_0}{1-\phi_1} \tag{105}$$

the dissolution process proceeds to completion (assuming that all the starch has the ability to dissolve). Using the values in Table 1a, dissolution completes if $W > 3$.

Common experience suggests this ratio is in the vicinity of 3.5 to achieve reasonable dissolution of rice grist in practice. We can conclude that this fairly simplistic model for surface dissolution is giving ratios in the correct region.

Results and discussion

In this section, the mass fraction of dissolved solids relative to the total mass of solids available is determined as a function of cooking time. The mass fraction is calculated using the ratio of $V_d(t)$ or $V_{td}(t)$ (where appropriate) to $4\pi(1-\phi_0)/3$. The cases of uniform grist size and of an arbitrary distribution of grist size are discussed under various cooking temperature regimes. The two effects (grist size and temperature history) are looked at individually and then in combination.

It will be assumed that changes in $T(t)$ are small enough to approximate D^* in (84) to unity. Furthermore we neglect any temperature dependence of ϕ_1 so a natural choice is $\phi_{ref} = \phi_1$ giving $\theta_s = 1$ and $\nu^* = \nu$. Under these conditions the temperature dependence only appears through $\theta_g(T)$.

A typical simple rule characterising the gelatinisation temperature (in °C) with moisture volume fraction, as illustrated in Figure 1, is

$$T_g = \begin{cases} 70 \quad , \quad \phi_g > 0.7 \\ 175 - 150\phi_g \quad , \quad \phi_g \leq 0.7 \end{cases} \quad . \tag{106}$$

In rescaled variables (using Table 1a parameter values), this equation can be rewritten as

$$\theta_g(T) = \frac{1}{90}\,(145 - T) \quad , \quad T \geq 70\,. \tag{107}$$

When all grist particles are the same size (scaled radius equal to unity), the mass fraction of dissolved solids increases with decreasing peeling thickness (or granule size) as shown in Figure 8. As discussed in the previous sections, the results of the continuous and discrete dissolution models are equivalent on identifying $\lambda = 2\Omega_2/\Delta$. Hence decreasing Δ is the same as increasing the dissolution rate.

The effect of having different but constant cooking temperatures is illustrated in Figure 9. When all grist particles are the same size, the mass fraction of dissolved solids increases with cooking temperature. Higher temperatures means that a lower moisture content is required for gelatinisation, resulting in a more rapid gelatinisation process. For both models, the dissolution speeds increase for higher temperatures.

We next explore the effect of changing the distribution of grist size on the total dissolved solids mass. (Note that the distributions are on a mass basis. To convert to a distribution based on the number of each size, it is necessary to divide by x^3 where x is the radius of the grist in the distribution.) Figure 10 shows the dissolved mass fraction as a function of time when the grist is made up of various proportions of two different masses. The results show that having smaller grist particles leads to more rapid dissolution. Furthermore, if there is a continuous distribution of grist sizes, Figure 11 shows that a 50/50 mixture

of two masses (curve (b)) can be accurately approximated for short and long times by continuous distributions which are weighted towards these two masses (curves (a) and (c) respectively).

Figure 13 shows the dissolution of a normal distribution of particle masses for the three temperature regimes illustrated in Figure 12. The curves show that as the temperature ramping steepens, the dissolved mass fraction increases more rapidly in the early stages. Figure 14 shows the effect of these different temperature regimes, when there are two grist masses. It exhibits the same qualitative behaviour as for the normal distribution case in Figure 13.

Conclusions

Several models have been developed to estimate analytic expressions for the total dissolved solids resulting from the cooking of rice grist. The processes modelled are water uptake and gelatinisation, followed by dissolution. The models are extended to account for a distribution of particle size and a changing process temperature.

An analytic solution has been determined using a Fickian diffusion model for water uptake and gelatinisation of a swelling spherical rice particle. Typically for cereal products, the moisture diffusivity is a strongly increasing function of moisture content and the diffusivity is much larger in gelatinised starch than ungelatinised starch. Consequently, as seen experimentally, there is a steep moisture front between the dry/ungelatinised and wet/gelatinised regions of a particle. Gelatinisation occurs at a certain moisture concentration, which is dependent on the temperature. It is a reasonable assumption then that gelatinisation occurs at the wetting front. In the absence of dissolution, this front moves so that its location is initially proportional to the square root of time, then becomes linear with time, and finally moves at a faster rate as it approaches the centre of the rice particle. The time for the entire piece of rice particle to be gelatinised has been calculated as a function of rice characteristics. These factors, which will change with rice variety, include

1. the moisture content at which the starch undergoes the irreversible gelatinisation reaction as a function of temperature,
2. the water diffusivity as a function of moisture content, and
3. initial and equilibrium moisture content.

Two new models (a discrete and a continuous model) have been presented that extend the above gelatinisation work to include the effects of the dissolution or peeling-away of cooked outer parts of the rice particle. These two models give a significant increase in the speed of the gelatinisation front and lead to linear front speeds over most of the

process. This type of linear penetration behaviour has been experimentally observed in many complex polymer systems, and has led other researchers (Thomas and Windle, 1982) to significantly modify Fickian models in an attempt to obtain linear behaviour. Our work presents a relatively simple extension of Fickian diffusion that is promising in that it exhibits these linear behaviours.

For the discrete dissolution model, we picture the rice particle interior to consist of concentric spherical shells of starch granules. The spherical shell of starch granules at the boundary, once ruptured by gelatinisation, is assumed to immediately peel away from the rice particle. The front speed depends on relevant gelatinisation parameters (temperature, moisture level and rice characteristics) and the thickness of the spherical shells which peel away. For the continuous dissolution model, we do not picture discrete starch layers peeling away instantaneously, but rather that the dissolution occurs continuously with time. For the continuous dissolution model with high dissolution rate, both the dissolution and gelatinisation fronts move at constant speed and there is a narrow gelatinised region between the fronts. The constant speed of these fronts is proportional to the dissolution rate, and inversely proportional to the thickness of the gelatinised region. The two approaches to the dissolution modelling can be made equivalent in a simple way.

The mass of rice solids released into solution is determined by using a constant velocity dissolution front, based on the analysis of the two dissolution models. As the dissolution proceeds, the rice particle radius reduces at a constant rate and the surface area reduces accordingly. The mass of dissolved solids, which initially increases rapidly, begins to level off giving reduced returns at later times. The dissolution process becomes less productive as time proceeds, which has implications for the optimal stopping time in production.

Extending these results to a consideration of the dissolved solids for a distribution of rice particle sizes reveals that smaller particles are dissolved more rapidly and hence the amount of dissolved solids initially rises faster than when all particles are the same size. The larger particles in the distribution take longer to dissolve and hence there is a more dramatic slow-down in total dissolved solids at later times. Everything in the modelling points to the fact that the dissolution process proceeds faster for small rice grist. However, in production, handling problems may arise when the grist size is too small.

Varying the temperature in the rice cooker influences the speed of the gelatinisation and dissolution fronts, and hence the amount of total dissolved solids at any given time. If the cost of cooking is calculated as a function of the temperature regime, this model can be used to optimise the temperature regime to lower energy costs. If a certain quantity of total dissolved solids is required, then various temperature regimes will give different processing times. These can be balanced against energy expenditure. The optimisation is complicated by the temperature dependence of both the diffusivity and gelatinisation moisture content, which will differ with rice variety.

A minimum water-to-rice ratio for complete starch dissolution was determined. Our anal-

ysis assumed that all of the available starch could be gelatinised and dissolved. This assumption may not be valid for some rice varieties.

Many factors and parameters influence the cooking process. Only some of these parameters are known for rice (grist size, initial moisture content). The models highlight the combinations of these parameters which are important for determining the rate of starch dissolution. The accurate determination of the diffusivity and its dependence on moisture content and the gelatinisation and equilibrium saturation moisture contents as a function of temperature is still needed for whole grain milled rice before the results in this paper can be confidently quantified.

Acknowledgements

This project arose from CUB BrewTech participation at the 1998 Mathematics-in-Industry Study Group, resulting in further collaboration between BrewTech, The University of Melbourne and Victoria University of Wellington. Malcolm Davey wishes to thank CUB BrewTech for its financial support of this project and the knowledge and input brought by Mr Tony Oliver and Dr Peter Rogers.

References

Bakshi A.S. and Sing R. P., " Modelling rice parboiling process", Lebensm Wiss u Technol, 15, 89-92 (1982).

Bear, J.,"Dynamics of Fluids in Porous Media," Dover, New York, (1972).

Beynum, G.M.A.van and Roels, J.A.,"Starch Conversion Technology," Marcel Dekker, New York, (1985).

Biliaderis, C. G., Page C.M., Maurice, T.J. and Juliano, B.O., "Thermal characterization of rice starches: A polymeric approach to phase transitions of granular starch", J. Agric. Food Chem, 34, 6-14 (1986).

de Gennes, P.G., "Scaling Concepts in Polymer Physics," Corwell University Press, London (1979).

Devotta, I., Ambeskar, V.D., Mandhare, A.B. and Mashelkar, R.A., "The Life time of a Dissolving Polymeric Particle," Chem. Eng. Sci., 49, 645-654 (1994a).

Devotta, I., Premnath, V., Badiger, M.V., Rajamohanan, P.R. and Mashelkar, R.A., "On the Dynamics of Mobilization in Selling-Dissolving Polymeric Systems," Macromolecules, 27, 532-539 (1994b).

Edwards, D.A. and Cohen, D.S., "A Mathematical Model for a Dissolving Polymer," AIChE J., 41, 2345-2355 (1995).

Fortes, M., Okos, M.R. and Barrett J.R., Heat and mass transfer analysis of intra-kernel wheat drying and rewetting," *J. Agric. Engng. Res.*, **26**, 109-125 (1981).

Gomi, Y., Fukuoka, M., Mihori, T. and Watanabe, H., "The rate of starch gelatinization as observed by PFG-NMR measurement of water diffusivity in rice starch/water mixtures", J Food Eng., 36, 359-369, (1998).

Herman, M.F. and Edwards, S.F., " A Reptation Model for Polymer Dissolution," Macromolecules, 23, 3662-3671 (1998).

Juliano, B.O., " Polysaccharides, proteins and lipids" in Rice: Chemistry and Technology", ed by Juliano, B.O., 2nd Edition, American Association of Cereal Chemists, St. Paul Minnesota, 59-174 (1985).

Juliano, B.O., "Criteria and tests for rice grain qualities", in Rice: Chemistry and Technology", ed by Juliano, B.O., 2nd Edition, American Association of Cereal Chemists, St. Paul Minnesota, 443-524 (1985).

Kar, N, Jain, R.K. and Srivastav, P.P., "Parboiling of dehusked rice", J Food Eng 39: 17-22 (1999).

Kirchoff, G., Vorlesungen uber die Theorie der Warme, Barth, Leipzig (1894).

Kunze, W., "Technology Brewing and Malting," 7th ed. (English Translation), VLB Berlin, (1996).

Kustermann, M., Scherer, R. and Kutzbach, H. D., Thermalconductivity and diffusivity of shelled corn and grain. *J. Food Process Eng*, **4**, 137-153 (1981).

Landman, K. A. and Please, C.P., "Modelling moisture uptake in a cereal grain," IMA J.Math App. In Bus. and Ind. 10: 265-287 (1999).

Landman, K.A., Pel, L. and Kaasschieter, E.F. "Analytic Modelling of Drying of Porous Materials", *Mathematical Engineering in Industry*, to appear 2000

Lund, D.B. and Wirakartakusumah, M., in "Engineering and Food, Proceedings of 3rd international Congress on Engineering and Food" ed. B.M. Mckenna, Elsevier Applied Science (1984).

McGowan, P. and McGuinness, M., "Modelling the cooking process of a single cereal grain," Proceedings of the Mathematics-in-Industry Study Group (John Hewitt, editor, 114-140 (1996).

McGuinness, M., Howlett, P. and Hong Jin, "Process Optimisation of Rice Gelatinisation for Beer Production", Proceedings of the Mathematics-in-Industry Study Group, ed J. Hewitt, 98-132 (1998).

McGuinness, M., Please, C.P., Fowkes, N., McGowan, P., Ryder, L. and Forte, D. "Modelling the Wetting and Cooking of a Single Cereal Grain," IMA J.Math App. In Bus. and Ind., 11, 49-70 (2000).

Papanu, J.S., Soane, D.S., Bell, A.T. and Hess, D.W., "Transport Models for Swelling and Dissolution of Thin Polymer Films," J. App. Sci., 38, 859-885 (1989).

Peppas, N.A., Wu, J.C. and Meerwall, E.D. von, "Mathematical Modeling and Experimental Characterization of Polymer Dissolution," Macromolecules, 27, 5626-5638 (1994).

Ramesh, M.N. and Srinivasa Rao P.N., "Development and performance evaluation of a continuous rice cooker", J Food Eng, 27, 377-387, (1996).

Ranade, V.V. and Mashelkar, R.A., "Convective Diffusion from a Dissolving Polymeric Particle," AIChE J., 41, 666-676 (1995).

Stapley, A. G. F., "Diffusion and Reaction in Wheat Grains," PhD Thesis, University of Cambridge, (1995).

Stapley, A.G.F., Fryer, P.J. and Gladden, L.F., "Diffusion and Reaction in Whole Wheat Grains during Boiling," AIChE J., 44, 1777-1789 (1998).

Suzuki, K., Kubota, K., Omichi. M. and Hosaka, H., "Kinetic Studies on Cooking of Rice," J. Food Sci., 41, 1180-1183 (1976).

Suzuki, K., Aki, M., Kubota, K. and Hosaka, H., "Studies on the Cooking Rate Equations of Rice," J. Food Sci., 42, 1545-1548 (1977).

Syarief, A.M., Gustafson, R.J. and Morey, R.V., "Moisture Diffusion Coefficients for Yellow-Dent Corn Components," Forum Pascasarjana, 9, 1-20 (1986).

Takeuchi, S., Fukuoka, M., Gomi, Y., Maeda, M. and Watanabe, H., " An application of magnetic resonance imaging to a real time measurement of the change of moisture profile in a rice grain during boiling ", J Food Eng, 33. 181-192 (1997a).

Takeuchi, S., Maeda, M., Gomi, Y., Fukuoka, M. and Watanabe, H., " The change of moisture distribution in a rice grain during boiling as observed by NMR imaging", J Food Eng, 33, 281-297 (1997b).

Tester, R.F. and Morrison, W.R., "Swelling and Gelatinization of Cereal Starches. I. Effects of Amylopectin, Amylose, and Lipids," Cereal Chemistry, 67, 551-557 (1990).

Thomas, N. L. and Windle, A.H., "A Theory of Case II diffusion," Polymer, 23, 529-542 (1982)

Whistler, R. L., Bemiller, J.N. and Paschall, E. F., "Starch: Chemistry and Technology," 2nd ed., Academic Press, New Yor, (1984).

Zhang, T, Bakshi, A.S., Gustafson, R.J. and Lund, D.B., "Finite element analysis od nonlinear water diffusion during rice soaking", J Food Sc. 49, 246-277 (1975).

Table 1a. Parameter values used for calculating water uptake and gelatinisation rates.

Constant	Value
initial mass (wet basis)	14%
initial rice density	1.43 g/l
ϕ_0	0.2
equilib. mass (wet basis)	73%
ϕ_1	0.8
c	5.22
ν	3.13
α	3

Table 1b. Parameter values as a function of θ_g

θ_g	Ω_1	Ω_2	VEF=$1+\frac{\Omega_1}{\Omega_2}$	t_g
0.2	0.88	1.47	1.6	0.13
0.3	0.85	0.95	1.9	0.22
0.4	0.81	0.68	2.2	0.31
0.5	0.76	0.51	2.5	0.43
0.6	0.68	0.38	2.8	0.59
0.7	0.58	0.28	3.1	0.83
0.8	0.45	0.19	3.4	1.28
0.9	0.26	0.10	3.7	2.54

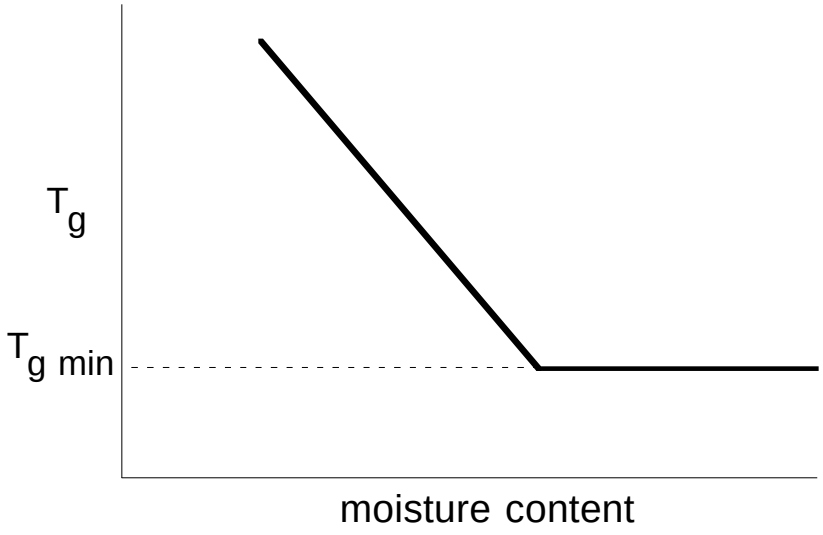

Figure 1: Schematic diagram of gelatinisation temperature versus moisture content.

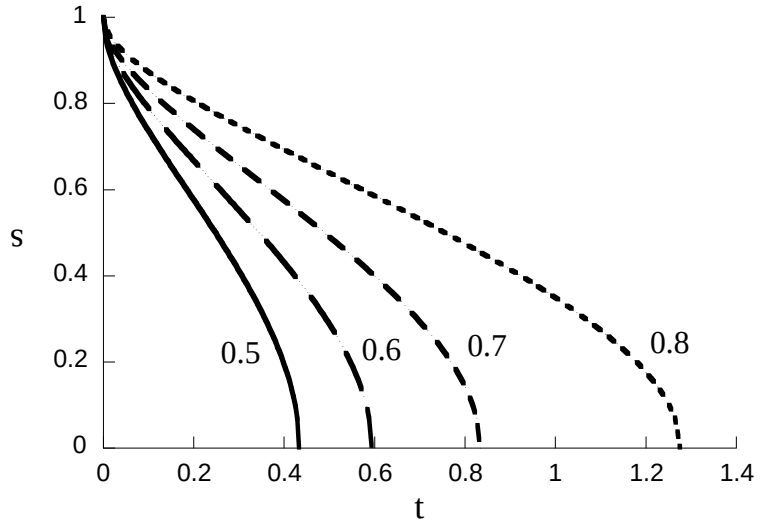

Figure 2: Plot of $s(t)$, using parameter values in Table 1a and various values of θ_g as shown.

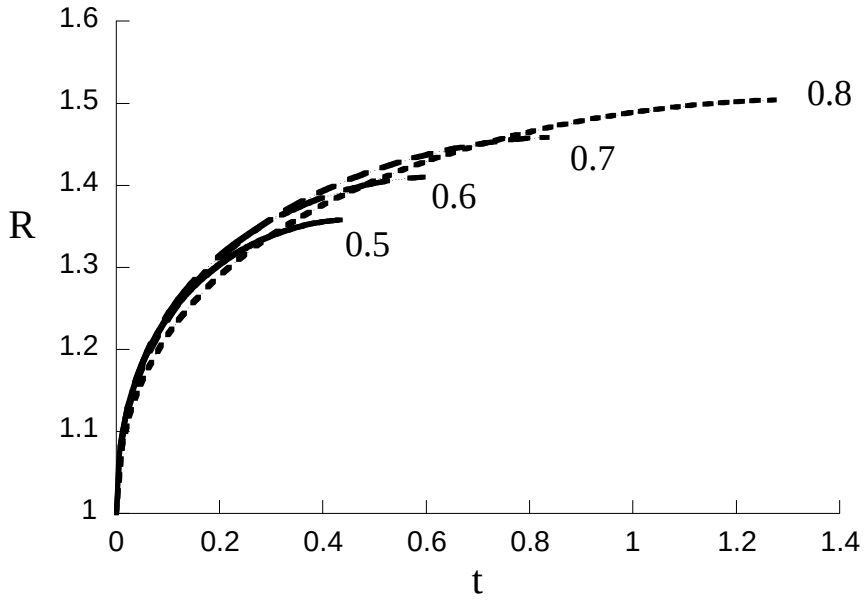

Figure 3: Plot of $R(t)$, using parameter values in Table 1a and various values of θ_g as shown.

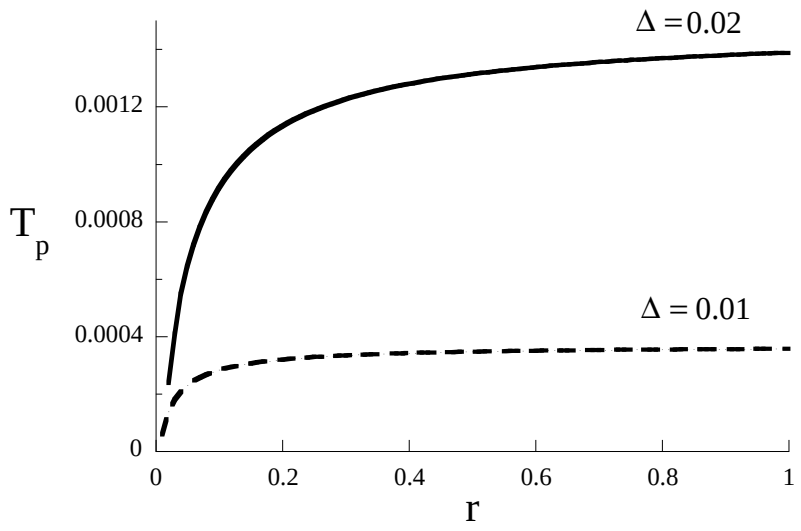

Figure 4: Plot of $T_{pr}(r, \Delta)$ versus r $(\Delta < r < 1)$, using parameter values in Table 1a, $\theta_g = 0.6$ and $\Delta = 0.01$ and 0.02.

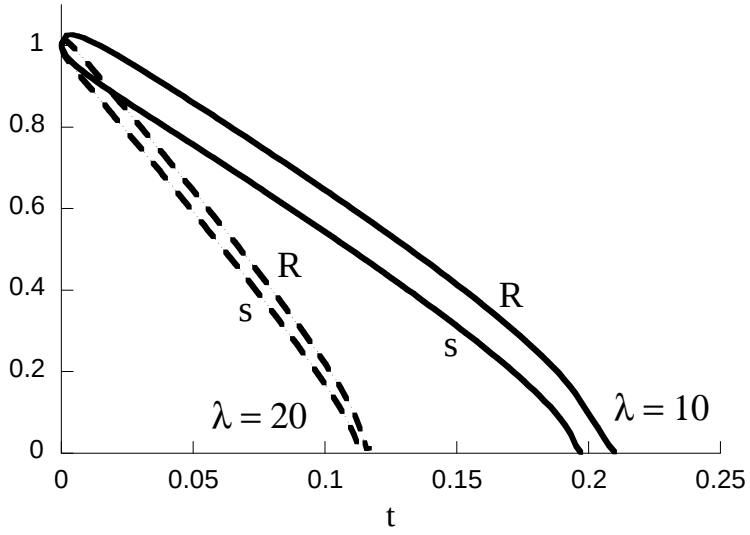

Figure 5: Plot of $R(t)$ and $s(t)$, using parameter values in Table 1a, $\theta_g = 0.6$ and $\lambda = 10$ and 20. Here $\lambda \gg \Omega_1 + \Omega_2 \approx 1.06$.

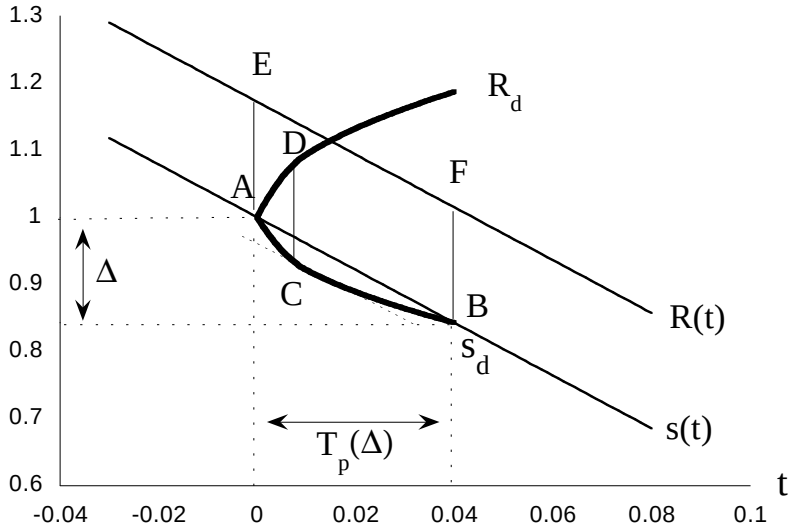

Figure 6: The equivalence of the discrete and continuous dissolution models.

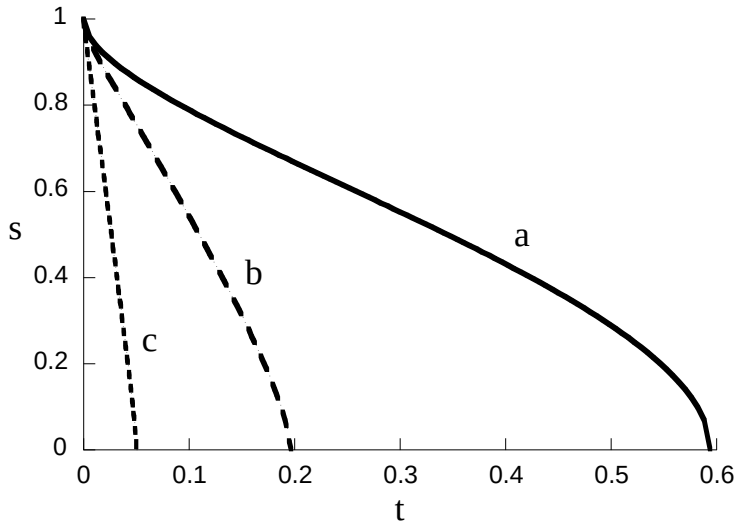

Figure 7: Comparison of $s(t)$ for (a) the no-dissolution model (b) the dissolution model with $\lambda = 10$ (c) the dissolution model with $\lambda = 50$. The parameter values are in Table 1a with $T = 91°\text{C}$ corresponding to $\theta_g = 0.6$.

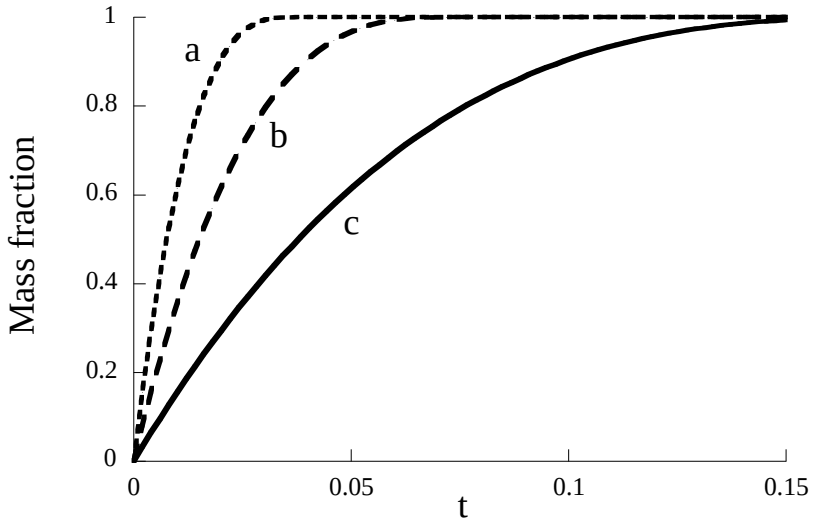

Figure 8: The mass fraction of dissolved starch versus time at different granule sizes Δ for grist with scaled radius unity; (a) $\Delta = 0.01$ (b) $\Delta = 0.02$ (c) $\Delta = 0.05$. The parameter values are in Table 1a $T = 91°\text{C}$ corresponding to $\theta_g = 0.6$.

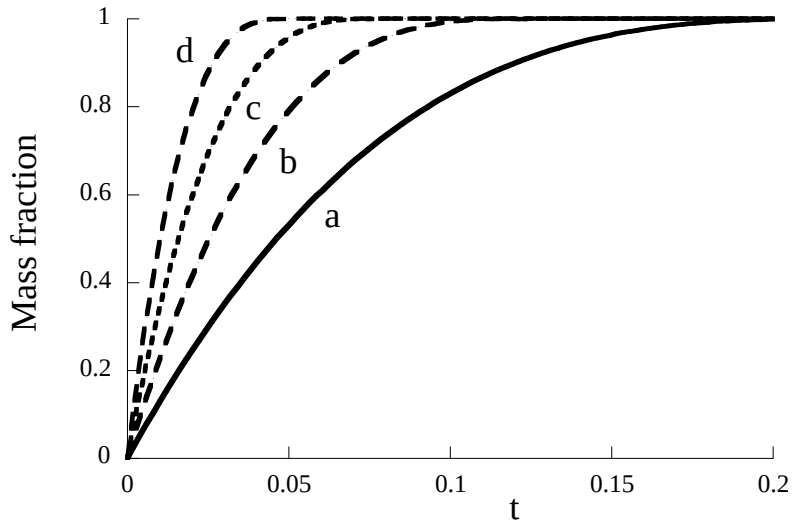

Figure 9: The mass fraction of dissolved starch versus time at different temperatures (in °C) for grist with scaled radius unity; (a) $T = 70$°C (b) $T = 80$°C (c) $T = 90$°C (d) $T = 100$°C. The parameter values are in Table 1a with $\Delta = 0.02$.

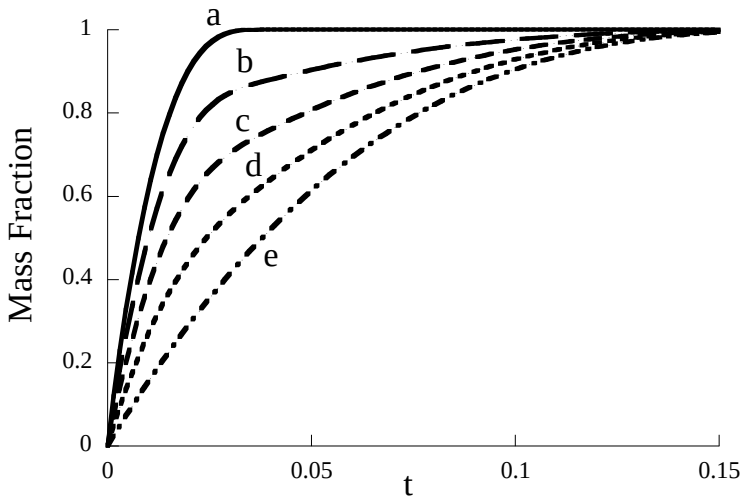

Figure 10: Starch mass fraction dissolved versus time for the following particle mass distributions: (a) every particle in the grist with scaled radius 0.5 (b) 3/4 of the mass of grist with scaled radius 0.5 and 1/4 of the mass of grist with scaled radius 2.5 (c) half the mass of grist with scaled radius 0.5 and half the mass of grist with scaled radius 2.5 (d) 1/4 of the mass of grist with scaled radius 0.5 and 3/4 of the mass of grist with scaled radius 2.5 (e) every particle in the grist with scaled radius 2.5. The parameter values are in Table 1a with $\Delta = 0.02$ and $T = 91°\text{C}$ corresponding to $\theta_g = 0.6$.

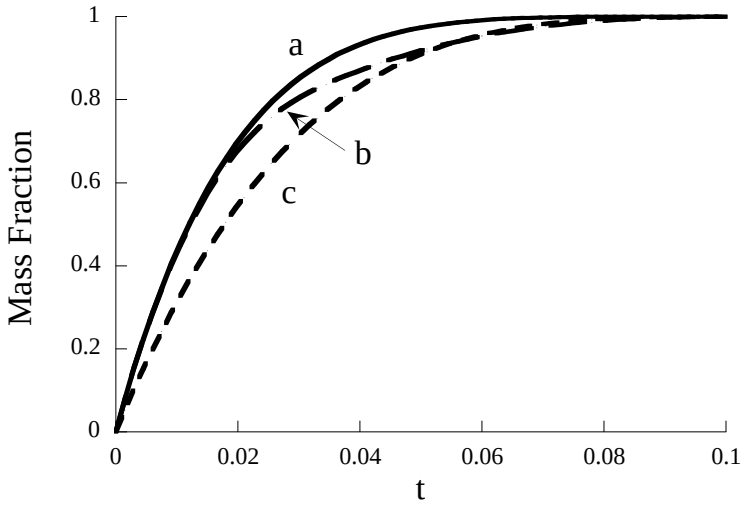

Figure 11: Starch mass fraction dissolved versus time for the following particle mass distributions: (a) mass distribution of $(1.5-x)^2x^3$, for $0.5 < x < 1.5$ (b) half the mass of grist with scaled radius 0.5 and half the mass of grist with scaled radius 1.5 (c) mass distribution of x^3, between $0.5 < x < 1.5$. The parameter values are in Table 1a with $\Delta = 0.02$ and $T = 91°\text{C}$ corresponding to $\theta_g = 0.6$.

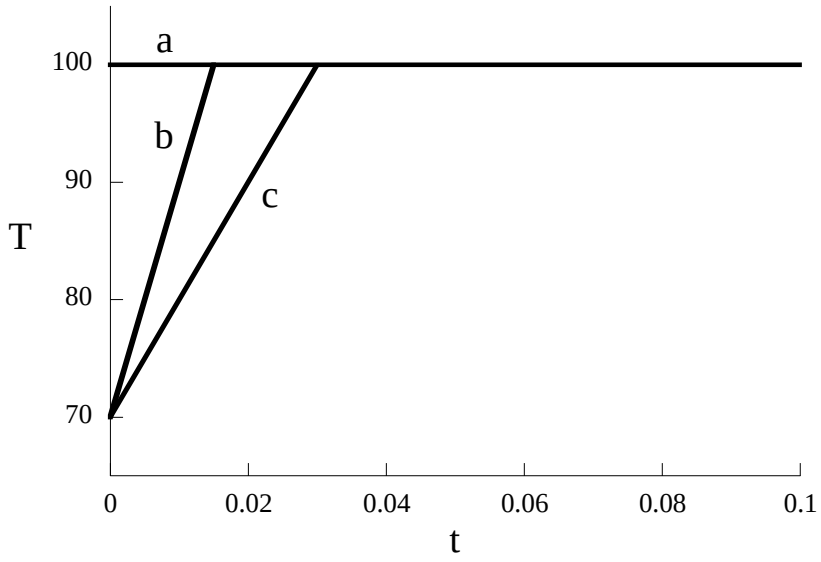

Figure 12: The temperature regime for the mass fractions shown in Figure 13 and Figure 14.

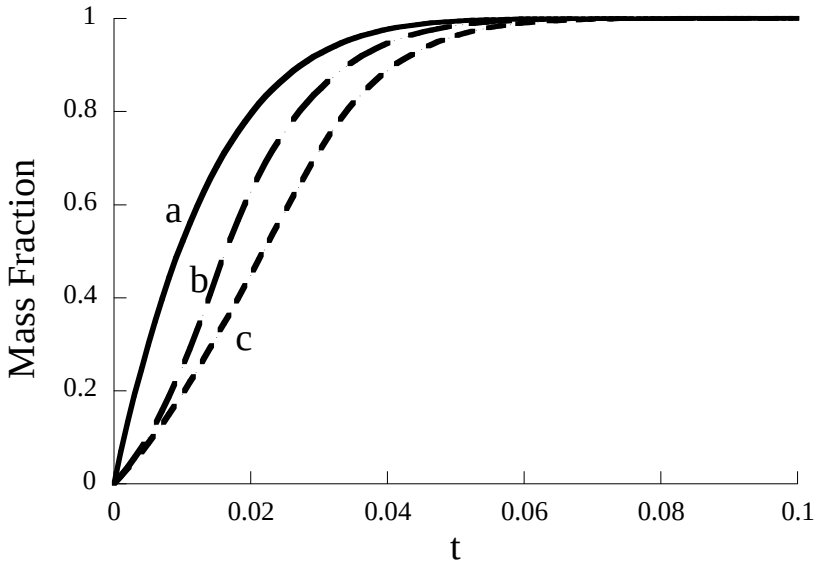

Figure 13: Starch mass fraction dissolved versus time for a normal mass distribution, mean $x = 1$, namely $e^{-5(x-1)^2}$, for $0.25 < x < 1.75$). The parameter values are in Table 1a with $\Delta = 0.02$ and equation (107). The three curves a, b, c correspond to the three different temperature regimes in Figure 12.

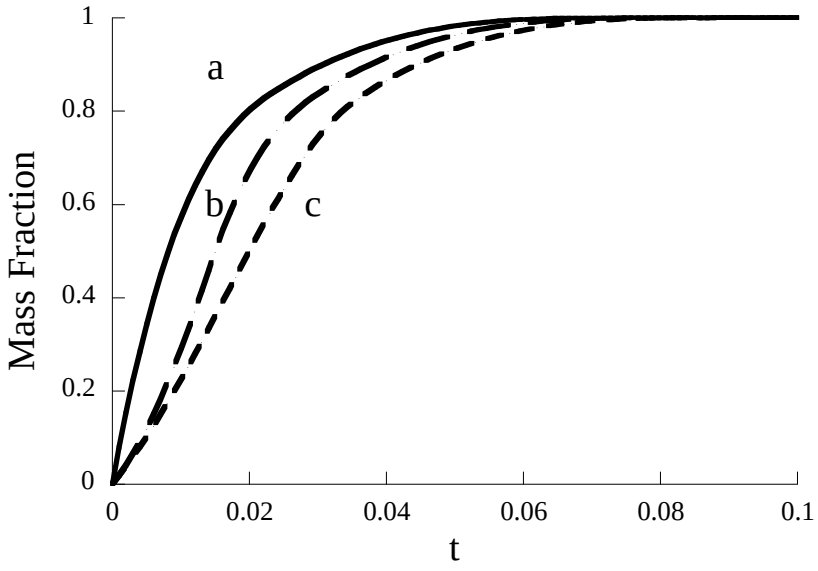

Figure 14: Starch mass fraction mass dissolved versus time where half the mass of grist with scaled radius 0.5 and the other half with scaled radius 1.5. The parameter values are in Table 1a with $\Delta = 0.02$ and equation (107). The three curves a, b, c correspond to the three different temperature regimes in Figure 12.